Atmos. Chem. Phys., 7, 6131–6144, 2007
www.atmos-chem-phys.net/7/6131/2007/


Atmospheric Chemistry and Physics

# Closure study between chemical composition and hygroscopic growth of aerosol particles during TORCH2

**M. Gysel[1,2], J. Crosier[1], D. O. Topping[1], J. D. Whitehead[1], K. N. Bower[1], M. J. Cubison[1,*], P. I. Williams[1], M. J. Flynn[1], G. B. McFiggans[1], and H. Coe[1]**

[1]Atmospheric Sciences Group, SEAES, University of Manchester, P.O. Box 88, Manchester, M60 1QD, UK
[2]Labor für Atmsphärenchemie, Paul Scherrer Institut, 5232 Villigen PSI, Switzerland
[*]now at: Cooperative Institute for Research in Environmental Sciences, University of Colorado, Boulder, CO 80309, USA

Received: 9 November 2006 – Published in Atmos. Chem. Phys. Discuss.: 5 December 2006
Revised: 24 September 2007 – Accepted: 22 November 2007 – Published: 14 December 2007

**Abstract.** Measurements of aerosol properties were made in aged polluted and clean background air masses encountered at the North Norfolk (UK) coastline as part of the TORCH2 field campaign in May 2004. Hygroscopic growth factors (GF) at 90% relative humidity (RH) for $D_0$=27–217 nm particles and size-resolved chemical composition were simultaneously measured using a Hygroscopicity Tandem Differential Mobility Analyser (HTDMA) and an Aerodyne aerosol mass spectrometer (Q-AMS), respectively. Both hygroscopic properties and chemical composition showed pronounced variability in time and with particles size. With this data set we could demonstrate that the Zdanovskii-Stokes-Robinson (ZSR) mixing rule combined with chemical composition data from the AMS makes accurate quantitative predictions of the mean GF of mixed atmospheric aerosol particles possible. In doing so it is crucial that chemical composition data are acquired with high resolution in both particle size and time, at least matching the actual variability of particle properties. The closure results indicate an ensemble GF of the organic fraction of $\sim$1.20$\pm$0.10 at 90% water activity. Thus the organics contribute somewhat to hygroscopic growth, particularly at small sizes, however the inorganic salts still dominate.

Furthermore it has been found that most likely substantial evaporation losses of $NH_4NO_3$ occurred within the HTDMA instrument, exacerbated by a long residence time of $\sim$1 min. Such an artefact is in agreement with our laboratory experiments and literature data for pure $NH_4NO_3$, both showing similar evaporation losses within HTDMAs with residence times of $\sim$1 min. Short residence times and low temperatures are hence recommended for HTDMAs in order to minimise such evaporation artefacts.

*Correspondence to:* M. Gysel
(martin.gysel@psi.ch)

## 1 Introduction

Atmospheric aerosols are typically hygroscopic such that water becomes the dominant component at high relative humidity (RH). This affects many interactions with the environment such as visibility degradation or direct and indirect climate effects. The ability of a particle to absorb water depends on its composition. Inorganic salts, organic matter, elemental carbon and mineral dust are major aerosol components and have been investigated in pure and mixed form in numerous studies and semi-empirical models predicting hygroscopic growth factors of multicomponent inorganic/organic particles are also available (ADDEM; Topping et al., 2005a,b). However, predicting the hygroscopicity of atmospheric aerosol particles based on their chemical composition is still a challenge since the composition depends on particle size, varies with time and comprises a vast number of different organic species. In earlier so-called "hygroscopicity closure" studies only the contribution to water uptake of the inorganic aerosol fraction was predicted, and the unexplained water uptake was then attributed to the organic fraction. In this way it has been found that the organic aerosol fraction most likely gives some contribution to hygroscopic growth (Saxena et al., 1995; Swietlicki et al., 1999; Dick et al., 2000), except for few studies of fresh urban particles, in which the organics rather appear to be inert with respect to water uptake (Saxena et al., 1995; Berg et al., 1998). Modest growth factors for the organic fraction, thus resulting in a minor contribution to overall water uptake, were confirmed in a closure study looking at extracts of the organic and the total water-soluble fractions from ambient filter samples (Gysel et al., 2004).

McFiggans et al. (2005) found, in a closure study including size-resolved composition and a detailed characterisation of the organic fraction as input for ADDEM predictions, that the variability in growth factor was largely dominated by the inorganic:organic mass ratio at any given size. Furthermore

Published by Copernicus Publications on behalf of the European Geosciences Union.

the water associated with the organic fraction was modest and relatively invariant between organics of different ensemble functional representations at two comparable locations. McFiggans et al. (2005) suggested further simplifying the treatment of the organic fraction into primary and secondary or aged contributions because determining the functional representation of the organic aerosol fraction as required for ADDEM is very costly and a limiting factor for both time and size resolution.

Recently, Aklilu et al. (2006) have combined highly time and size resolved chemical composition data obtained by an Aerodyne Quadrupole Aerosol Mass Spectrometer (Q-AMS; Jayne et al., 2000) with simplified model calculations applying the Zdanovskii-Stokes-Robinson (ZSR) mixing rule (Zdanovskii, 1948; Stokes and Robinson, 1966) and a constant organic growth factor. In agreement with the expectations expressed by McFiggans et al. (2005) they achieved reasonably good closure against Hygroscopicity Tandem Differential Mobility Analyser (HTDMA) measurements when sulphate was the dominant inorganic compound. However, in the presence of nitrate the predictions clearly overestimated the growth. Therefore they speculated that either the ZSR mixing rule does not hold for particles containing ammonium nitrate or that in their case the nitrate detected by the Q-AMS may have originated from organic nitrates instead of ammonium nitrate.

In this study we applied a similar approach using Q-AMS data and ZSR modelling against HTDMA measurements within the second field experiment of the UK NERC-funded Tropospheric ORganic CHemistry project (TORCH2) in a location encountering predominantly aged air masses. We also found that closure is only achieved in the absence of significant nitrate loadings. Based on a larger data set covering a wider size range, we can state the hypotheses that the ZSR mixing rule is sufficiently accurate for GF predictions and that the disagreement is likely to be caused by a nitrate evaporation artefact in the HTDMA.

## 2 Experimental and data analysis

### 2.1 Sampling site and instrumentation

Measurements were conducted in May 2004 as part of the second Tropospheric ORganic CHemistry (TORCH2) field campaign at the Weybourne Atmospheric Observatory (WAO, 52°57′02″ N, 1°07′19″ E), which is located on the North Norfolk coastline near Weybourne, UK. Air masses encountered at this station represent aged polluted outflow from London, the West Midlands or the European continent for large scale wind directions south, west, or east, respectively, or relatively clean air masses transported across the North Sea region by northerly wind. North Norfolk is a sparsely populated rural region without large population centres or industrial areas.

Air was drawn down a 150 mm bore, 12 m high sampling stack at a flow rate of $150\,\mathrm{l\,min^{-1}}$ and then sub-sampled through a 40 mm bore stainless steel line running into the container, where the HTDMA and the Q-AMS were connected next to each other.

A HTDMA was used to measure hygroscopic growth factor distributions at 90% RH of particles with dry diameters $D_0$ between 27–217 nm. The hygroscopic growth factor of a particle is defined as $g(\mathrm{RH})=D(\mathrm{RH})/D_0$, where $D(\mathrm{RH})$ is the diameter at a fixed RH. The first Differential Mobility Analyser (DMA) was operated with dried sheath air and a cylindrical volume with a residence time of ∼60 s was included between the humidifier and the second DMA. More details can be found in Cubison et al. (2005). Atmospheric particles of a defined dry size typically exhibit a range of growth factors or even clearly separated growth modes, because of external mixing or variable relative fractions of different compounds in individual particles (hereinafter referred to as quasi-internally mixed). Growth factor probability distributions $c(g)=dC/dg$ are retrieved from each measurement, and normalised such that $C=\int c(g)\,dg=1$. The inversion method applied to the raw data (Gysel et al., 2007[1]) has similarities to the OEM inversion algorithm described by Cubison et al. (2005). The distribution $c(g)$ is also inverted from the measurement distribution into contributions from fixed classes of narrow growth factor ranges, but instead of using a linear inversion, $c(g)$ is fitted to the actual measurements using a full TDMA transfer forward model.

The RH in the second DMA ($\mathrm{RH_{DMA2}}$) generally reached the target of 90% within ±1% but for occasional larger drifts. In order to minimise the effect of $\mathrm{RH_{DMA2}}$ drifts, all growth factors measured between 88 and 92% RH were corrected to 90% RH. An empirical hygroscopicity parameter ($k$) was first determined from the measured growth factor and the actual RH, with which the corresponding growth factor at 90% RH could then be calculated. The empirical growth parametrisation used is given in Eq. (4) of the paper by Gysel et al. (2004) with $k=(M_w\cdot\rho_s\cdot i_s)/(\rho_w\cdot M_s)$.

An Aerodyne Q-AMS (Jayne et al., 2000) was used to provide on-line, quantitative measurements of the chemical composition and mass size distributions of the non-refractory fine particulate matter ($\mathrm{NR\text{-}PM_1}$) at a high temporal resolution. The Q-AMS was alternating between two operation modes: (i) in the mass-spectrum (MS) mode the averaged chemical composition of the $\mathrm{NR\text{-}PM_1}$ aerosol ensemble is determined without size resolved information, (ii) in time-of-flight (ToF) mode the *m/z* of key chemical components can be resolved as a function of the vacuum aerodynamic diameter of the particles. More detailed descriptions of the Q-AMS measurement principles and various calibrations (Jayne et al., 2000), its modes of operation (Jimenez

[1]Gysel, M., McFiggans, G. B., Coe, H., et al.: Inversion of tandem differential mobility analyser (TDMA) measurements, in preparation, 2007.

**Table 1.** Density and growth factors of all compounds used in the hygroscopicity closure (Topping et al., 2005a).

| | Density $\rho$ [ $\mathrm{kg\,m^{-3}}$] | $g$(RH=90%) $D_0$=60 nm [-] | $g$(RH=90%) $D_0$=137 nm [-] | $g$(RH=90%) $D_0$=217 nm [-] | $g(a_w$=0.9) $D_0=\infty$ [-] |
|---|---|---|---|---|---|
| $(NH_4)_2SO_4$ | 1769 | 1.66 | 1.70 | 1.72 | 1.73 |
| $NH_4HSO_4$ | 1780 | 1.74 | 1.78 | 1.80 | 1.81 |
| $H_2SO_4$ | 1830 | 2.02[a] | 2.05[a] | 2.06[a] | 2.07[a] |
| $NH_4NO_3$ | 1720 | 1.74 | 1.80 | 1.82 | 1.83 |
| Organics | 1400[b] | 1.16[c] | 1.18[c] | 1.19[c] | 1.20[c] |

[a] Sulphuric acid is expected to retain water at 5–10% RH corresponding to a growth factor of ∼1.15, which is taken into account when calculating the mixed particle growth factor at 90% RH.
[b] The density of organics was chosen to represent oxidised organics in aged atmospheric aerosol (Alfarra et al., 2006; Dinar et al., 2006).
[c] The organic growth factor $g_{\mathrm{org}}(a_w$=0.9) was fitted for best hygroscopicity closure results and corresponding $g_{\mathrm{org}}$(RH=90%) for all dry sizes were calculated assuming surface tension of pure water.

et al., 2003) and data processing and analysis (Allan et al., 2003, 2004) are available. The main chemical components measured by the Q-AMS are $SO_4^{2-}$, $NO_3^-$, $NH_4^+$ and organics, while refractory compounds such as elemental carbon, mineral dust, sodium chloride and sodium sulphate are not detected.

A dual Differential Mobility Particle Sizer (DMPS) system comprising a short and a long Vienna type DMA in combination with a TSI 3025 and 3010 Condensation Particle Counter (CPC), respectively, was used to measure particle number size distributions from 4 to 827 nm. Total particle number concentrations were measured with an additional CPC Model TSI 3025.

### 2.2 Hygroscopic growth predictions

Growth factor predictions based on chemical composition are made using the ZSR mixing rule (Zdanovskii, 1948; Stokes and Robinson, 1966). The ZSR mixing rule for mixtures is equivalent to linear interpolation of the water uptake in between the water uptake of pure substances. For hygroscopic growth factors it can be written as:

$$g_{\mathrm{mixed}}(a_w) \approx \left( \sum_i \varepsilon_i g_i(a_w)^3 \right)^{\frac{1}{3}}, \quad (1)$$

where $a_w$ is the water activity, $g_{\mathrm{mixed}}$ is the growth factor of the mixed particle, $g_i$ are the growth factors of the compounds in pure form, $\varepsilon_i$ are the volume fractions of the compounds in the dry particle, and the summation is performed over all compounds. The Köhler equation, RH= $a_w \cdot S_k$, describes the equilibrium RH for a solution droplet, where $S_k$ is the Kelvin factor. Using the Köhler equation and Eq. (1) to calculate $g_{\mathrm{mixed}}$(RH), requires an iterative algorithm because $S_k$ depends on the droplet size and thus on $g_{\mathrm{mixed}}$. However, $g_{\mathrm{mixed}}$(RH) can be directly obtained in good approximation by replacing $a_w$ with RH in Eq. (1).

The Q-AMS mainly measures $SO_4^{2-}$, $NO_3^-$, $NH_4^+$ and organics, while the ZSR relation requires volume fractions and hygroscopic growth factors of neutral salts and the organics as input. Reilly and Wood (1969) have introduced an ion pairing scheme, which is a commonly accepted method to calculate the neutral salts from the molar numbers of all ions. However, the Reilly and Wood scheme requires an iterative algorithm for acidic systems. Therefore we use a simplified ion pairing scheme with a direct analytical solution:

$$\begin{aligned} n_{NH_4NO_3} &= n_{NO_3^-} \\ n_{H_2SO_4} &= \max(0, n_{SO_4^{2-}} - n_{NH_4^+} + n_{NO_3^-}) \\ n_{NH_4HSO_4} &= \min(2n_{SO_4^{2-}} - n_{NH_4^+} + n_{NO_3^-}, \\ &\qquad n_{NH_4^+} - n_{NO_3^-}) \\ n_{(NH_4)_2SO_4} &= \max(n_{NH_4^+} - n_{NO_3^-} - n_{SO_4^{2-}}, 0) \\ n_{HNO_3} &= 0 \quad , \end{aligned} \quad (2)$$

where $n$ denotes the number of moles. The above scheme (Eq. 2) and the Reilly and Wood scheme give identical results if the aerosol is fully neutralised by $NH_4^+$, because $NH_4NO_3$ and $(NH_4)_2SO_4$ are the only possible salts. The deviations of the corresponding ZSR-predictions from ADDEM (Topping et al., 2005a) are $\Delta g/g \leq 1\%$ at 90% RH for all nitrate to sulphate ratios. For the $H^+$-$NH_4^+$-$HSO_4^-$-$SO_4^{2-}$-$H_2O$ system the above scheme (Eq. 2) makes a piecewise linear interpolation of the water uptake between the pure substances $(NH_4)_2SO_4$ and $NH_4HSO_4$, and between $NH_4HSO_4$ and $H_2SO_4$ for ammonium to sulphate ratios larger and smaller than unity, respectively. This scheme gives slightly more accurate ZSR predictions ($\Delta g/g \leq 2\%$) than the Reilly and Wood scheme ($\Delta g/g \leq 4\%$). Making up the ion balance with only $(NH_4)_2SO_4$ and $H_2SO_4$ would result in $\Delta g/g \leq 6\%$. Sometimes the size-resolved Q-AMS data indicate presence of $NO_3^-$ in incompletely neutralised aerosol (see Sect. 3.3). Also in these cases the above scheme provides slightly more accurate water uptake predictions ($\Delta g/g \leq 1\%$) than the

Reilly and Wood scheme ($\Delta g/g \leq 3\%$) for the composition range encountered during TORCH2.

Volume fractions $\varepsilon_i$ of the inorganic salts and the organics are obtained from respective dry densities and mass fractions delivered by the Q-AMS assuming volume additivity. Growth factors $g_i$ of all inorganic salts were obtained from ADDEM and an ensemble value of $g_{\text{org}}$=1.20 at $a_w$=0.9 was used for the organic fraction (see Table 1). This particular value of $g_{\text{org}}$ was chosen because it delivered best closure results as detailed in Sect. 3.5.

The ZSR relation (Eq. 1) shows that the growth factor of a mixed particle is largely driven by the relative abundance (expressed by $\varepsilon_i$) of more and less hygroscopic compounds. Furthermore the mixed particle growth factor is more sensitive to uncertainties in growth factors of more hygroscopic compounds than of less hygroscopic compounds, which can be seen from the partial derivative by $\partial g_i$ of Eq. (1):

$$\frac{\partial g_{\text{mixed}}}{\partial g_i} = \frac{\varepsilon_i g_i^2}{g_{\text{mixed}}^2}. \quad (3)$$

For a two compound particle with pure growth factors of $g_1$=1.20 and $g_2$=1.80, as an example, the critical volume fraction of compound 1 above which $g_{\text{mixed}}$ is more sensitive to $g_1$ than to $g_2$ is as high as $g_1^2/(g_1^2+g_2^2)$=0.69. Therefore the speciation of inorganic salts is normally more important than detailed characterisation of the organic fraction.

## 3 Results and discussion

### 3.1 Air mass origin

The beginning of the measurement period (8–10 May) was characterised by frequent cloud cover, some rainfall and air masses originating from continental Europe and transported across the North Sea (five-day back trajectories from the ECWMF). From 11–13 May clean air masses originating from the Norwegian Sea or the Northeastern Atlantic Ocean were transported across the North Sea to the WAO without land contact for several days. During the period from 14–20 May the weather was dry and virtually cloud free, the wind speeds were low and air masses originated from the Northeastern Atlantic Ocean and were transported across Ireland and North England or the English Midlands. However, during this period the local wind speed showed a diurnal pattern which is not captured by the back trajectories, most probably a sea breeze effect, with wind from the north during the day and wind from the south during the night. From 21–23 May again clean air masses from the Northeastern Atlantic Ocean were transported across the North Sea to the site with possibly some land contact over northern Scotland. In the following the flow regimes described above will be referred to as "aged polluted 1" (8–10 May), "clean marine 1" (11–13 May), "aged polluted 2" (14–20 May), and "clean marine 2" (21–23 May).

### 3.2 Hygroscopic behaviour

Growth factor distributions $c(g)$ (see Sect. 2) along with the volumetric mean growth factor and the number fraction of particles with growth factor larger than 1.15 ($N_{g>1.15}$) are shown in Fig. 1 with a time resolution of 1 h. Generally a strong influence of particle size and air mass type was observed. The events "clean marine 1" and "clean marine 2" were very similar, the growth factors at all dry sizes showed little variation over time and a single narrow growth mode was observed, indicating that the particles were quasi-internally mixed with limited differences in composition between individual particles. As an exception around 10% of the observed particles at $D_0$=217 nm during the "clean marine 2" event were non-hygroscopic in nature, which might be the remains of some short land contact over Scotland or from ship traffic in the North Sea. It is worth noting that no externally mixed sea salt particles with growth factors larger than 2 have been found in the investigated size ranges. The observations during the "aged polluted 1" event, where the air arrived from continental Europe across the North Sea, showed a slightly lower mean growth factor than that observed in the marine events, but like the latter showed a dominant single hygroscopic mode. The "aged polluted 2" event, influenced by more recent pollution over England, clearly showed a different picture: particles with dry sizes $D_0 \geq 89$ nm were externally mixed with a small fraction of non-hygroscopic particles ($g \approx 1.0$) and a main mode of particles with growth factors varying between 1.3 and 1.6. The main growth mode, containing around 80 to 90% of the particles, was generally narrow though occasionally a clear spread of growth factors or even a third mode was observed. The mean growth factor of particles with $D_0 \leq 60$ nm, varied between 1.2 and 1.6, which is also the reason for the strong variations of $N_{g>1.15}$ for small particles. Completely non-hygroscopic particles were not observed in this size range and there was no clearly detectable separation into distinct modes, though there was often a clear spread of growth factors in the main mode. This indicates that the small particles were quasi-internally mixed, i.e. the fractional contribution of different compounds varied between individual particles. The variations of growth factors and $N_{g>1.15}$ showed a diurnal pattern strongly linked to the local wind direction with a minimum in mean growth factor and $N_{g>1.15}$ after midnight and a maximum in mean growth factor and $N_{g>1.15}$ after noon.

### 3.3 Particle number, mass and chemical composition

A CPC and a DMPS were used to measure the total particle number concentration and the particle number size distribution, respectively ($D$=4–827 nm). Figure 2a shows that the integrated number particle concentration from the DMPS size distribution agrees well with the direct measurement from the CPC. Panel a) also shows the integrated number

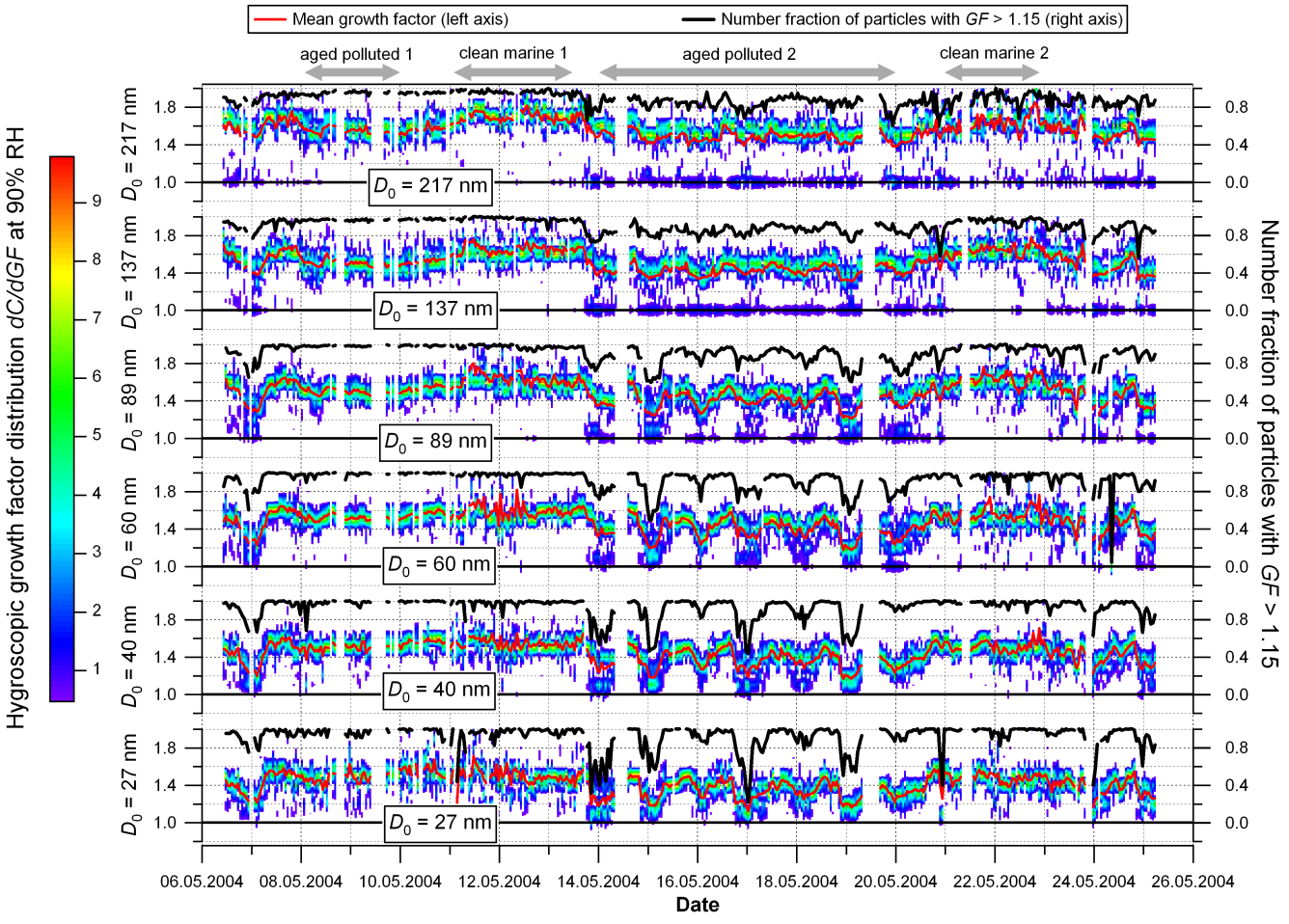


**Fig. 1.** Growth factor probability distributions for different particle dry sizes as measured with a HTDMA. The red lines represent the $3^{rd}$-moment mean growth factors, black lines the number fraction of particles with $g > 1.15$.

of particles with diameters larger than 55 nm in order to provide a rough distinction between ultrafine and accumulation mode particles. The total particle number concentration varied massively from $<500$ to $>20\,000\,\mathrm{cm}^{-3}$. Lowest number concentrations were observed during the two "clean marine" events, whereas highest number concentration peaks observed during the "aged polluted 2" and "clean marine 2" events were most probably a result of recent nucleation events, as can be seen from the clear dominance of particles with diameters smaller than 55 nm.

The number size distributions have also been used to estimate the total fine aerosol mass by multiplication of the total integrated volume by a density of $1600\,\mathrm{kg\,m}^{-3}$ (see below for discussion of particle density). In Fig. 2b the "DMPS-mass" is compared with the total NR-$PM_1$ detected by the Q-AMS. The Q-AMS masses have been derived using a collection efficiency of 0.5 as has been commonly observed in many previous experiments (Drewnick et al., 2005). The bias of the Q-AMS mass relative to the DMPS mass is shown in Fig. 2c. The agreement between DMPS and Q-AMS mass is generally good, confirming proper instrument operation. Exceptions with a clearly positive Q-AMS mass bias are marked by orange ellipses in Fig. 2b,c). Systematic positive bias occurred always if the aerosol was either very acidic or if the nitrate mass fraction was greater than ∼40%. This indicates that in these cases the Q-AMS collection efficiency was most likely greater than 0.5 (Crosier et al., 2007). Thus the reported Q-AMS data are probably over-corrected for collection efficiency in these events. Absence of substantial negative biases also indicates that the refractory material, which is not detected by the Q-AMS, is probably only a minor fraction. Whilst other more standard techniques for determination of the chemical speciation of submicron aerosol were not available, the mass loadings reported here are consistent between the total AMS mass and the DMPS derived mass over a wide range of relative concentrations of the key species. The Q-AMS and DMPS data indicate total fine mass loadings of 5–10, <5, 5–15, and $<3\,\mu\mathrm{g\,m}^{-3}$ for the events "aged

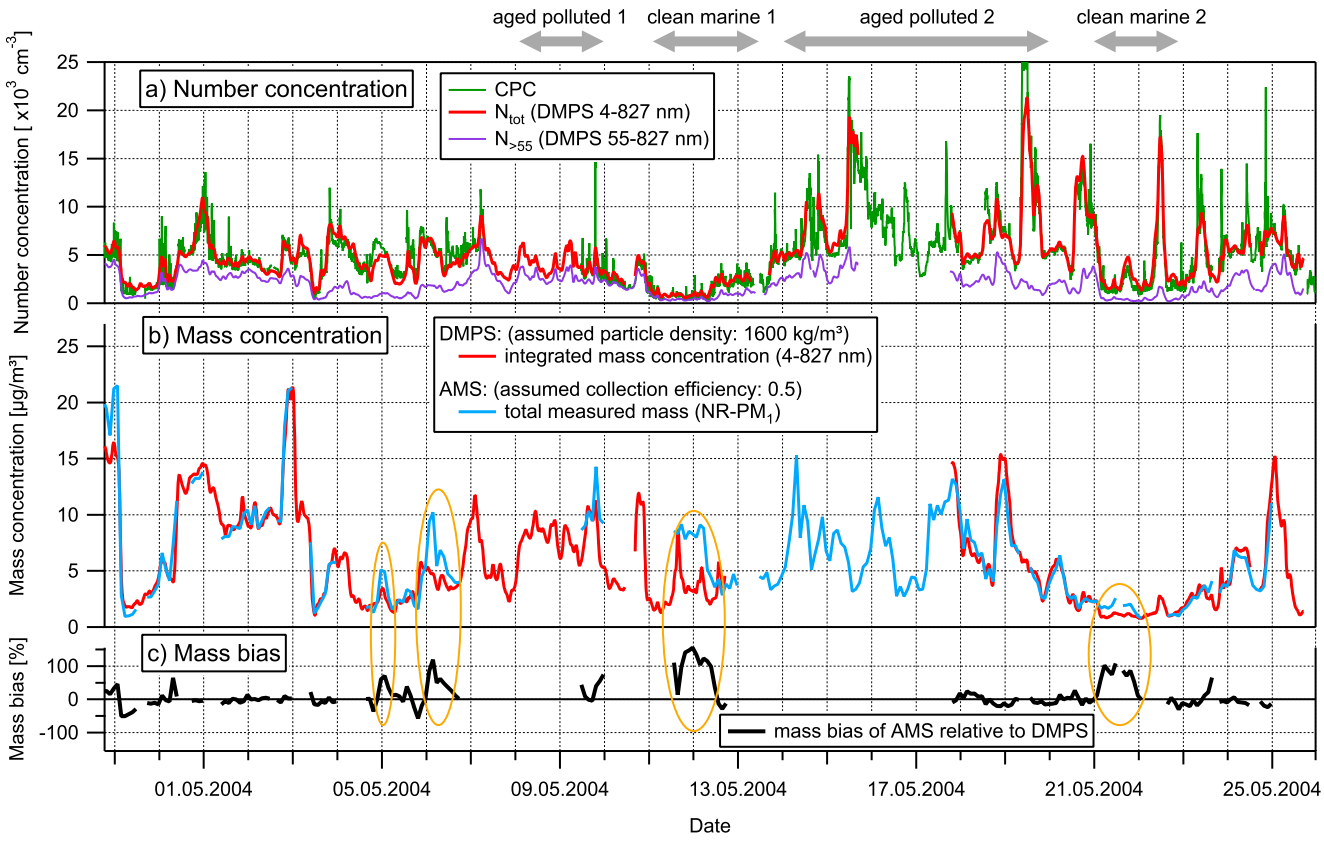


**Fig. 2.** Instrument comparison of number concentration from CPC and integrated DMPS **(a)**, mass loadings derived from DMPS and Q-AMS **(b)**, and bias of Q-AMS relative to DMPS **(c)**. Orange ellipses indicate periods where Q-AMS and DMPS disagree substantially. All disagreements occurred when the aerosol was either very acidic or had a high nitrate content, probably resulting in a higher collection efficiency of the Q-AMS. This means that the Q-AMS mass loadings are probably overcorrected in these periods by applying a collection efficiency of only 0.5 as has been done.

polluted 1", "clean marine 1", "aged polluted 2", and "clean marine 2", respectively.

Time and size dependent chemical composition from the Q-AMS is shown as relative contributions to the total detected mass (Fig. 3). Panel a) shows the integrated composition of the NR-$PM_1$ as measured in the MS-mode, while panels b) to d) show size resolved data obtained in the ToF-mode integrated over the size ranges 68–145, 145–309, and 309–659 nm vacuum aerodynamic diameter, respectively. These ranges correspond to centre mobility diameters of 66, 141, and 301 nm assuming spherical particles and a density of 1500, 1600, and 1600 kg $m^{-3}$, respectively. Mixed particle density values are based on the typical chemical composition observed and assuming a density of 1400 kg $m^{-3}$ for the organic fraction (Alfarra et al., 2006; Dinar et al., 2006, see also Table 1).

The two "clean marine" events are characterised by ~80% of sulphates and ~20% organics, while there is no nitrate present nor is there a pronounced size dependence of the composition. The measured $NH_4^+$ concentration was often insufficient to fully neutralise $SO_4^{2-}$, indicating an acidic aerosol. This is reasonable for trajectories without land contact for five days.

During the "aged polluted 2" event there was, similar to the hygroscopic behaviour, a distinct diurnal pattern strongly linked with the local wind direction. Particularly sulphate and nitrate exhibited an opposite trend of maxima during daytime and nighttime, respectively. However, the total inorganic fraction remained fairly constant with around 60–80%, 40–60%, and 10–50%, in the (mobility) diameter bins 301, 141, and 66 nm respectively. Consequently also the organic fraction was fairly constant with around 20–40%, 40–60%, and 50–90% in the respective size bins. In the presence of $NO_3^-$ the measured $NH_4^+$ concentration was sufficient to fully neutralise $NO_3^-$ and $SO_4^{2-}$ (top panel of Fig. 3), as is to be expected. However, sometimes the size-resolved data (lower panels of Fig. 3) indicate presence of $NO_3^-$ in incompletely neutralised aerosol, which is caused by limited measurement statistics in narrow size ranges and by averaging over finite time intervals.

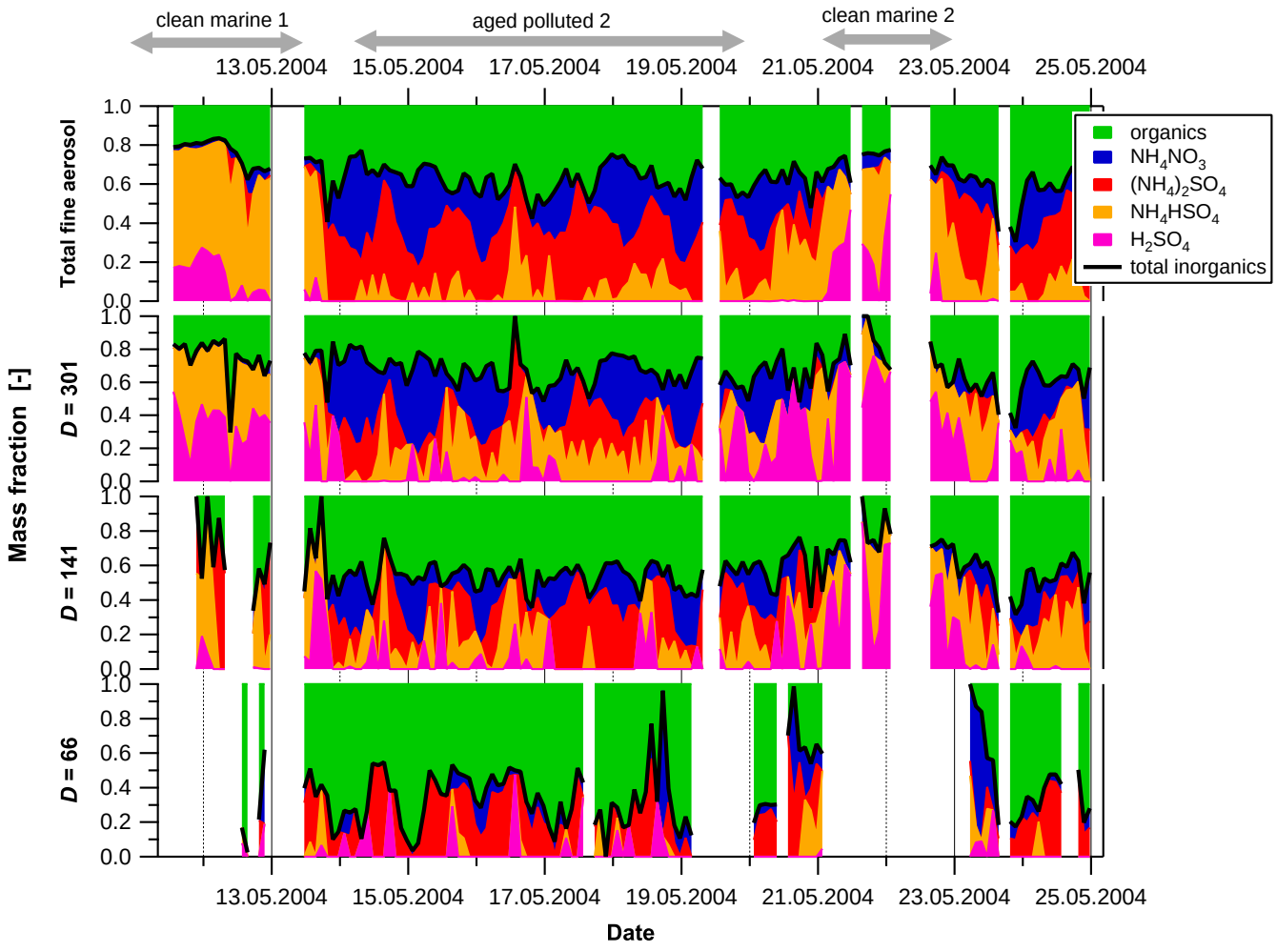


**Fig. 3.** Composition of non-refractory compounds as measured by the Q-AMS for the total fine aerosol and for different size ranges.

### 3.4 Hygroscopicity closure

Successful hygroscopicity closure is achieved if high correlation and a mean ratio of ∼1 between measurement and prediction is found, or in other words, if the prediction bias has a limited scatter about zero. The AMS/ZSR prediction approach used here is described in Sect. 2.2. It has to be added that the 3rd-moment mean growth factor of the HTDMA's growth factor distributions is compared with the predicted values because the Q-AMS provides the average composition of all particles of a given size without any information on the mixing state.

The TORCH2 data set shows pronounced size dependence and temporal variability of chemical composition and hygroscopic properties, which confirms the need to make the hygroscopicity closure with high temporal and size resolution. Otherwise high correlation between measurement and predictions might just result from averaging out positive and negative deviations occurring at shorter time scales or smaller size intervals.

A time series of measured and predicted mean growth factors at different dry sizes is shown in the top three panels of Fig. 4 with a time resolution of 2 h. It has to be emphasised at the outset that the AMS/ZSR predictions shown here take an evaporation artefact of ∼61% of the $NH_4NO_3$ within the HTDMA instrument into account as detailed in Sect. 3.6. The blue line shows the AMS/ZSR prediction when using an ensemble growth factor of $g_{org}$=1.20 at $a_w$=0.9 in the AMS/ZSR predictions. Additional comparisons between the HTDMA measurement and this AMS/ZSR prediction are shown as prediction bias (bottom panel of Fig. 4) and correlation plots (left hand side panels of Fig. 5). The prediction bias scatters about the zero line and it is smaller than 5% for most data points. Correspondingly the coefficient of determination is as high as $r^2$≈0.43–0.47 at different sizes, and the fitted slopes are very close to unity for $D_0$=137 and 217 nm particles. Some systematic deviation is only found for $D_0$=60 nm with a fitted slope of 0.84. However, particularly during the "clean marine" events the signal statistics in this size bin were often at the lower limit, most probably

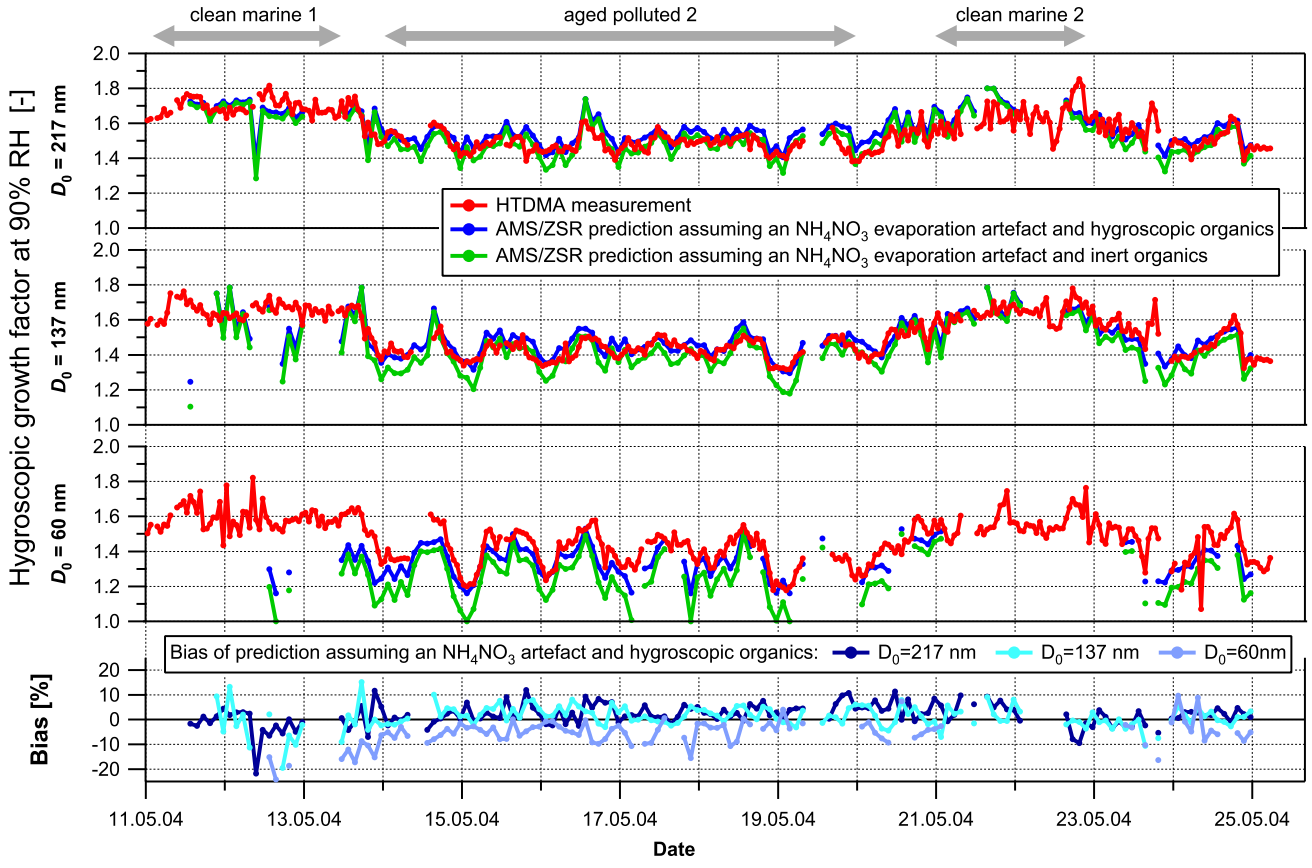


**Fig. 4.** Size-resolved hygroscopicity closure between HTDMA measurement and growth factor predictions using the ZSR relation with chemical composition according to Q-AMS data. The AMS/ZSR predictions include the assumption that an $NH_4NO_3$ evaporation artefact occurred in the HTDMA. For the organics an ensemble growth factor of $g_{org}$=1.20 (hygroscopic) and $g_{org}$=1.0 (inert) at $a_w$=0.9 was used for the two predictions shown as blue and green lines, respectively. The bottom panel shows the bias of the AMS/ZSR prediction using hygroscopic organics relative to the HTDMA measurement.

leading to a couple of points with overestimated organic mass fraction, since the Q-AMS's organic mass is the sum of many different *m/z* fragments with a very low signal to noise ratio. In summary we can state that the combination of AMS chemical composition data with the ZSR mixing rule including a simplified treatment of the organic fraction makes reasonably accurate predictions of mean growth factors with high time and size resolution possible for atmospheric particles in aged air masses.

The Q-AMS cannot detect refractory material such as sodium chloride and sodium sulphate, which are found in particles containing sea salt and have growth factors of 2.41 and 1.92 at $a_w$=0.9, respectively (ADDEM; Topping et al., 2005a). Thus not considering either of them in the ZSR model would lead to a strong underprediction of growth factors. Sea salt particles are found in marine air masses with larger number fractions along with high wind speeds and at larger sizes, though HTDMA studies often report only low frequency of occurrence and small number fractions at diameters below 200 nm even in marine air masses (McFiggans et al., 2006). In this study it is unlikely that sodium chloride and sodium sulphate were present in significant amounts in the investigated size range since neither a systematic underprediction of growth factors nor externally mixed particles with growth factors above 2 were observed in the marine air masses.

### 3.5 Growth factor of the organics

Best results in the hygroscopicity closure (blue lines in Fig. 4) were obtained with an ensemble growth factor of $g_{org}$=1.20 at $a_w$=0.9 for the organics (see Table 1 for corresponding size dependent growth factors at RH=90%). The green lines in Fig. 4 correspond to AMS/ZSR predictions using $g_{org}$=1.0 at 90% RH, which is a lower limit value. Comparing the blue and green lines shows that reducing $g_{org}$ has little effect on predicted growth factors in the range $g \geq 1.45$, whereas they clearly decrease in the range $g \leq 1.45$. It has

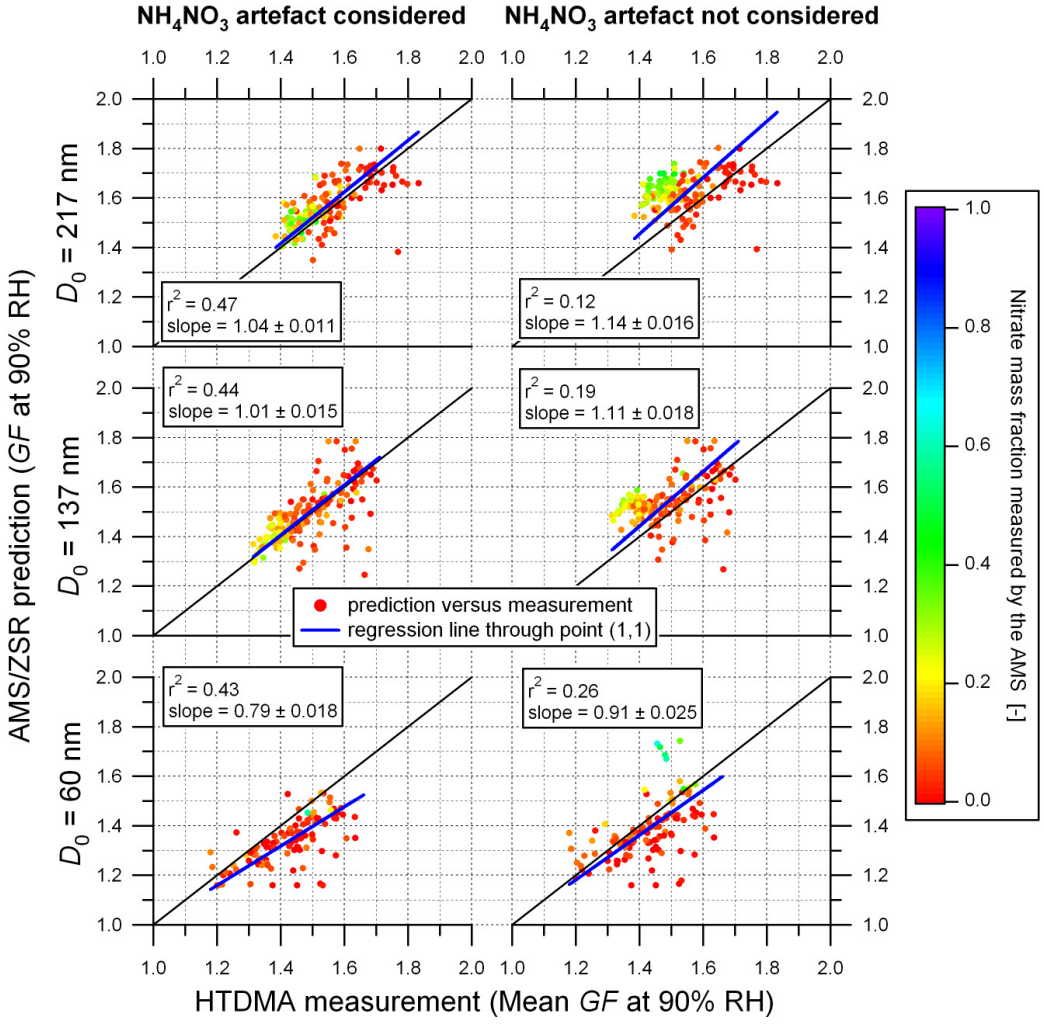


**Fig. 5.** Scatter plot of AMS/ZSR prediction versus HTDMA measurements for different dry sizes ("rows"). For the AMS/ZSR predictions shown on the left hand side panels it was assumed that an $NH_4NO_3$ evaporation artefact occurred in the HTDMA instrument, whereas no artefact was assumed for the predictions shown on the right hand side panels. Regression lines (blue) are fitted through the point (1.0, 1.0). The colour code of the data points indicates the measured nitrate mass fraction.

already been pointed out in Sect. 2.2 that growth factors of mixed inorganic/organic particles are only sensitive to $g_{org}$ if the organics dominate. The assumption of $g_{org}$=1.0 results in systematic underprediction of growth factors in the latter cases, which is mostly seen at the smallest size. Therefore we can conclude the ensemble GF of the organics is about $g_{org} \approx 1.20 \pm 0.10$ at 90% water activity.

In a previous hygroscopicity closure study on ambient aerosol at two different sites Aklilu et al. (2006) inferred organic growth factors at 80% RH of 1.03–1.04 and 1.11–1.14 during periods influenced by urban emission and dominated by secondary particulate matter, respectively. These values roughly translate to 1.07–1.09 and 1.22–1.28 at 90% RH. Carrico et al. (2005) have shown that the growth factor of the organics in carbonaceous matter dominated and biomass burning influenced aerosol in the Yosemite National Park is in the order of 1.11–1.16 at 80% RH, which corresponds to about 1.22–1.30 at 90% RH. Hygroscopic growth factors at 90% RH of humic-like substances isolated from ambient filter samples have been reported to be ∼1.18 (Gysel et al., 2004). McFiggans et al. (2005) have calculated a growth factor of ∼1.11 at 90% RH for organic model compounds according to H-NMR functional group analysis of organics from ambient filter samples. Secondary organic aerosol formed by photooxidation of volatile organic precursors in smog chamber experiments has been found to have a growth factor of ∼1.11 at 85% RH, which corresponds to about 1.17 at 90% RH (Baltensperger et al.,

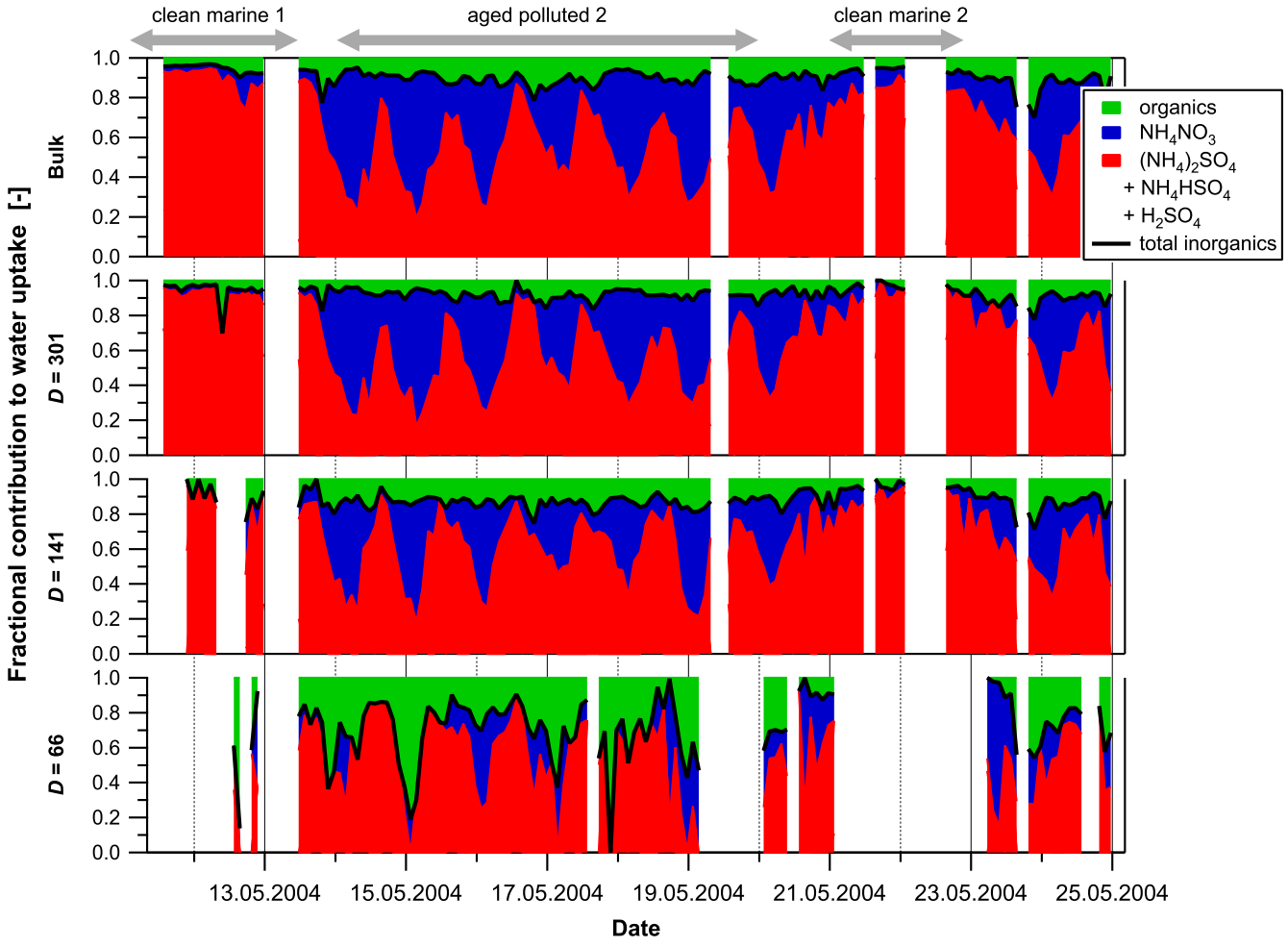


**Fig. 6.** Fractional contribution of major compounds to hygroscopic water uptake at 90% RH as calculated from the Q-AMS chemical composition. Total fine aerosol **(a)**, and particles with dry mobility diameters of around 301 **(b)**, 141 **(c)**, and 66 nm **(d)**.

2005). Some multifunctional organic acids have been shown to have growth factors of ∼1.46 (Peng et al., 2001), whereas e.g. fatty acids and alkanes have growth factors of 1.0 at 90% RH, though neither of the latter two compound classes is expected to dominate the organics in aged atmospheric aerosol. A growth factor of about $g_{org}$≈1.20±0.10 at $a_w$=0.9 inferred in this study agrees with the above literature, bearing in mind that oxygenated organic species (OOA) dominated over hydrocarbon-like organic species (HOA) in the aged air masses encountered during TORCH2 (Zhang et al., 2007).

The AMS/ZSR predictions using $g_{org}$=1.20 show that the contribution of the organics to the overall water uptake is mostly of minor importance, as illustrated in Fig. 6. The inorganic compounds completely dominate the water uptake at 137 and 217 nm with more than 80 and 90% fractional contribution, respectively. Of the inorganic salts sulphate vastly dominates during the "clean marine" events, while $NH_4NO_3$ is comparably important during the "aged polluted" events. The organic contribution to the hygroscopic growth of particles in the size range $D$≥137 nm is always very minor (Fig. 6) even though its contribution to the mass is ∼20–60% (Fig. 3). Only at 60 nm, where the organic mass fraction is ∼50–90%, the fractional contribution of the organics to the water uptake reaches ∼20–50%.

### 3.6 $NH_4NO_3$ evaporation artefact

The right hand side panels in Fig. 5 show the correlation between measured and predicted mean growth factors, whereas the chemical composition obtained by the AMS is fully considered including $NH_4NO_3$. The colour code indicates the mass fraction of nitrate relative to the total mass detected by the Q-AMS in the respective size ranges. While the points with low nitrate mass fractions (reddish colours) scatter about the 1:1-line, the points with high nitrate mass fractions (greenish colours) stand out with systematically

overpredicted growth factors (or too low measurements). This bias of 10% and more is particularly well seen at $D$=137 and 217 nm, but also for the few points with high nitrate at $D$=60 nm.

Particulate $NH_4NO_3$ is well known to cause negative (evaporation) or positive (sorption) artefacts in various aerosol sampling techniques. Mikhailov et al. (2004) have observed RH-dependent evaporation losses for pure $NH_4NO_3$ particles of up to 27 vol% during a residence time of ∼11 s in their HTDMA. This is in line with our own laboratory experiments, where an evaporation loss of up to 15–35 vol% was measured with two HTDMAs both having a residence time of ∼20 s. Furthermore, in a HTDMA operated at 20°C and with a residence time of ∼1 min we have found evaporation losses of >65 vol% at RH=20% and 50–60 vol% at RH=90% for pure $D$=100 and 50 nm $NH_4NO_3$ particles, respectively. Dassios and Pandis (1999) reported evaporation times of ∼0.5, 1, and 5 min for pure $D$=100, 200, and 500 nm $NH_4NO_3$ particles, respectively, using a TDMA set up with a laminar flow evaporation cell at room temperature. They have also shown that evaporation rates increase with increasing temperature.

In the ambient measurements of this study the aerosol experienced first changes in the sampling line, where it was heated up from ambient temperature (∼10–18°C) to laboratory temperature (24–26°C). Thus a fraction of $NH_4NO_3$ may have been lost in the inlet system, but obviously not completely according to the Q-AMS measurements. Evaporation losses of $NH_4NO_3$ in the Q-AMS instrument itself are minimal. On the other hand some evaporation losses are likely to occur in the HTDMA, which had a residence time of ∼60 s. Good closure can be achieved (blue lines in Fig. 4 and left hand side panels in Fig. 5), if either the mass fraction of $NH_4NO_3$ is assumed to be zero (complete evaporation from the particles before they enter DMA1), or alternatively if ∼61% of $NH_4NO_3$ is assumed to evaporate from the particles after DMA1. In the AMS/ZSR predictions taking $NH_4NO_3$ evaporation into account it is assumed that the water content on the particles passing through DMA2 is in equilibrium with the $NH_4NO_3$ and other compounds remaining on the particles. This modified AMS/ZSR prediction considering the $NH_4NO_3$ artefact increases the coefficient of determination at different sizes from $r^2$≈0.12–0.26 up to $r^2$≈0.43–0.47, and brings the data points with high nitrate mass fraction down to the 1:1-line. The estimate for the $NH_4NO_3$ evaporation artefact of ∼61% has been obtained with a least square fit. However, tuning this number could not be used to trim the closure results ad libitum because a single value was used in the AMS/ZSR predictions for all sizes and times.

Most of the evaporation artefact is likely to occur within the HTDMA instrument between DMA1 and DMA2 according to the evaporation time scales of pure $NH_4NO_3$ in TDMA instruments. Based on the above discussion we conclude that an $NH_4NO_3$ evaporation artefact occurred in the HTDMA instrument and we recommend to apply short residence times in HTDMA instruments and to keep sampling line temperatures low. An implication of the above findings is that any HTDMA measurement applying long residence times to ambient particles might suffer from an $NH_4NO_3$ artefact if not otherwise proven, and that measured growth factors might be considerably smaller than what they would be for undisturbed ambient particles.

Also Aklilu et al. (2006) found good agreement between HTDMA measurement and AMS/ZSR prediction in a similar hygroscopicity closure study, except for periods when nitrate was present and growth factors were overpredicted. They have speculated that either the ZSR relation might not hold for mixtures containing $NH_4NO_3$ or that some nitrate may have been in the from of organic nitrates, but they have not considered the possibility of evaporative $NH_4NO_3$ losses in the HTDMA. However, the accuracy of ZSR predictions of growth factors is better than ±3% for mixed electrolytes of atmospheric importance (see Sect. 2.2 and Topping et al., 2005a), and Marcolli and Krieger (2006) have shown that electrolyte/organic interactions hardly influence the water activity for a range of organics mixed with NaCl, $(NH_4)_2SO_4$ or $NH_4NO_3$, i.e. that the ZSR rule can be applied with small errors. Therefore the discrepancies found in this study can most likely not solely be attributed to inaccuracy of the ZSR mixing rule. It is also unlikely that the nitrates detected in our study originate mostly from organic nitrates instead of $NH_4NO_3$, because the relative intensity of the fragments $m/z$ 30 ($NO^+$) and $m/z$ 46 ($NO_2^+$) in the mass spectrum is constantly ∼3, which is the characteristic value of $NH_4NO_3$. Furthermore in the presence of nitrate, ion balance is achieved for $NH_4^+$, $NO_3^-$ and $SO_4^{2-}$, if $NO_3^-$ is assumed to be from $NH_4NO_3$.

The Q-AMS cannot detect elemental carbon (EC), which is not hygroscopic in pure form (Weingartner et al., 1997). Not considering EC in the ZSR model results in an overprediction of growth factors, however, the observed discrepancies could only be explained with assuming EC mass fractions in the fine aerosol of up to ∼40%, which would be extremely high for an aged aerosol (Krivácsy et al., 2001; Putaud et al., 2004) and thus cannot be expected. Furthermore, the fragment $m/z$ 57, which has been shown to correlate well with EC under strong influence from primary emissions (Zhang et al., 2005a,b), shows good correlation with the number fractions of non-hygroscopic particles at 217 and 137 nm ($r^2$=0.30 at 137 nm). Assuming that these particles are soot particles composed of EC and primary organics translates into reasonable ratios of $m/z$ 57 to EC. The influence of non-hygroscopic particles on the mean growth factor is only minor because their number fraction hardly exceeds 20% (Fig. 1), thus confirming that EC is very unlikely to be the main reason for the observed discrepancies.

The Q-AMS's signal intensity depends on the collection efficiency, the fraction of a species successfully vaporised on the heater, and the ionisation efficiency. Collection

efficiencies less than unity in the AMS are thought to be a result of particle bounce on the heater, and so affect all species in the bouncing particle equally (Matthew et al., 2007[2]). The collection efficiency of $NH_4NO_3$ is expected to be equal to the other compounds because the measured growth distributions indicate internal mixture of nitrate with sulphate and organics (Fig. 1). Furthermore, comparison of the AMS mass with the DMPS derived mass indicates that a substantial increase of the collection efficiency in the presence of $NH_4NO_3$ only occurred for very few data points with $NH_4NO_3$ mass fractions greater than ∼40%. It is possible that the collection efficiency can vary with time due to variations in composition. This does not affect ZSR predictions made with sufficiently high time resolution, because only mass fractions are required, which are independent of the collection efficiency for internally mixed particles. A small part of the observed overprediction could be caused by an overestimation of the $NH_4NO_3$ mass fraction. However, it can be ruled out as the sole reason because closure is only achieved by reducing the $NH_4NO_3$ mass fraction down to zero (see above).

Temporal variations of the ensemble growth factor of the organics can be ruled out as a reason for the observed discrepancies because the sensitivity of predicted growth factors is too small, which also applies to a number of minor assumptions regarding particle density, volume additivity, or shape factors.

## 4 Conclusions

Chemical composition and hygroscopic growth factors of aerosol particles in aged air masses have been investigated and the ZSR mixing rule was used to predict hygroscopic growth factors based on chemical composition. The major outcomes of this closure study are:

- The ZSR mixing rule combined with chemical composition data from the AMS makes accurate quantitative predictions of the mean GF of mixed atmospheric aerosol particles possible.
- Chemical composition data must be acquired with high resolution in both particle size and time, at least matching the actual variability of particle properties.
- The organics can be described with an ensemble growth factor of $g_{org}$=1.20±0.10 at $a_w$=0.9.
- More sophisticated thermodynamic models do not improve the closure since the uncertainties in the measurements are the limiting factor, specifically if the required composition data cannot be acquired with sufficient time and size resolution.
- The inorganic fraction dominates the hygroscopic water uptake at high RH with a fractional contribution of more than 80% at $D \geq 137$ nm, whereas the organic contribution to water uptake is minor (<20% at $D \geq 137$ nm), except for organic-dominated 60 nm-particles.
- The closure results strongly indicate a substantial $NH_4NO_3$ evaporation artefact within the HTDMA when nitrate is present (residence time ∼1 min). A positive prediction bias due to overestimation of the $NH_4NO_3$ mass fraction is very unlikely to be the sole reason for the observed discrepancies.
- Laboratory experiments and literature data with pure $NH_4NO_3$ particles show substantial evaporation artefacts in HTDMAs when residence times are ∼1 min, while they are moderate when residence times are ∼10 s.
- Short residence times and low temperatures are recommended in HTDMAs in order to minimise evaporation artefacts.

*Acknowledgements.* We thank for financial support of this work by the Swiss National Science Foundation and by the British Natural Environment Research Council through grant number NER/T/S/2002/00494. We also thank B. Bandy from the University of East Anglia for providing the meteorological parameters for the WAO station.

Edited by: S. Martin

## References

Aklilu, Y., Mozurkewich, M., Prenni, A. J., Kreidenweis, S. M., Alfarra, M. R., Allan, J. D., Anlauf, K., Brook, J., Leaitch, W. R., Sharma, S., Boudries, H., and Worsnop, D. R.: Hygroscopicity of particles at two rural, urban influenced sites during Pacific 2001: Comparison with estimates of water uptake from particle composition, Atmos. Env., 40, 2650–2661, 2006.

Alfarra, M. R., Paulsen, D., Gysel, M., Garforth, A. A., Dommen, J., Prévôt, A. S. H., Worsnop, D. R., Baltensperger, U., and Coe, H.: A mass spectrometric study of secondary organic aerosols formed from the photooxidation of anthropogenic and biogenic precursors in a reaction chamber, Atmos. Chem. Phys., 6, 5279–5293, 2006, http://www.atmos-chem-phys.net/6/5279/2006/.

Allan, J. D., Jimenez, J. L., Williams, P. I., Alfarra, M. R., Bower, K. N., Jayne, J. T., Coe, H., and Worsnop, D. R.: Quantitative sampling using an Aerodyne aerosol mass spectrometer 1. Techniques of data interpretation and error analysis, J. Geophys. Res, 108, 4090, doi:10.1029/2002JD002358, 2003.

Allan, J. D., Bower, K. N., Coe, H., Boudries, H., Jayne, J. T., Canagaratna, M. R., Millet, D. B., Goldstein, A. H., Quinn, P. K., Weber, R. J., and Worsnop, D. R.: Submicron aerosol

[2]Matthew, B.M. and Onasch, T.B., and Middlebrook, A.M.: Collection efficiencies in an Aerodyne aerosol mass spectrometer as a function of particle phase for laboratory generated aerosols, Aerosol Sci. Technol., submitted, 2007.

composition at Trinidad Head, California, during ITCT 2K2: Its relationship with gas phase volatile organic carbon and assessment of instrument performance, J. Geophys. Res, 109, D23S24, doi:10.1029/2003JD004208, 2004.

Baltensperger, U., Kalberer, M., Dommen, J., Paulsen, D., Alfarra, M. R., Coe, H., Fisseha, R., Gascho, A., Gysel, M., Nyeki, S., Sax, M., Steinbacher, M., Prevot, A. S. H., Sjögren, S., Weingartner, E., and Zenobi, R.: Secondary organic aerosols from anthropogenic and biogenic precursors, Faraday Discuss., 130, 265–278, 2005.

Berg, O. H., Swietlicki, E., Frank, G., Martinsson, B. G., Cederfelt, S. I., Laj, P., Ricci, L., Berner, A., Dusek, U., Galambos, Z., Mesfin, N., Yuskiewicz, B., Wiedensohler, A., Stratmann, F., and Orsini, D.: Comparison of observed and modeled hygroscopic behavior of atmospheric particles, Contr. Atmos. Phys., 71, 47–64, 1998.

Carrico, C. M., Kreidenweis, S. M., Malm, W. C., Day, D. E., Lee, T., Carrillo, J., McMeeking, G. R., and Collett Jr., J. L.: Hygroscopic growth behavior of a carbon-dominated aerosol in Yosemite National Park, Atmos. Env., 39, 1393–1404, 2005.

Crosier, J., Allan, J. D., Coe, H., Bower, K. N., Formenti, P., and Williams, P. I.: Chemical composition of summertime aerosol in the Po Valley (Italy), Northern Adriatic and Black Sea, Quart. J. Roy. Meteorol. Soc., 133, 61–75, 2007.

Cubison, M., Coe, H., and Gysel, M.: Retrieval of hygroscopic tandem DMA measurements using an optimal estimation method., J. Aerosol Sci., 36, 846–865, 2005.

Dassios, K. G. and Pandis, S. N.: The mass accommodation coefficient of ammonium nitrate aerosol, Atmos. Env., 33, 2993–3003, 1999.

Dick, W. D., Saxena, P., and McMurry, P. H.: Estimation of water uptake by organic compounds in submicron aerosols measured during the Southeastern Aerosol and Visibility Study, J. Geophys. Res, 105, 1471–1479, 2000.

Dinar, E., Mentel, T. F., and Rudich, Y.: The density of humic acids and humic like substances (HULIS) from fresh and aged wood burning and pollution aerosol particles, Atmos. Chem. Phys., 6, 5213–5224, 2006,
http://www.atmos-chem-phys.net/6/5213/2006/.

Drewnick, F., Hings, S. S., DeCarlo, P., Jayne, J. T., Gonin, M., Fuhrer, K., Weimer, S., Jimenez, J. L., Demerjian, K. L., Borrmann, S., and Worsnop, D. R.: A new time-of-flight aerosol mass spectrometer (TOF-AMS) - Instrument description and first field deployment, Aerosol Sci. Technol., 39, 637–658, 2005.

Gysel, M., Nyeki, S., Paulsen, D., Weingartner, E., Baltensperger, U., Galambos, I., and Kiss, G.: Hygroscopic properties of water-soluble matter and humic-like organics in atmospheric fine aerosol, Atmos. Chem. Phys., 4, 35–50, 2004,
http://www.atmos-chem-phys.net/4/35/2004/.

Jayne, J. T., Leard, D. C., Zhang, X. F., Davidovits, P., Smith, K. A., Kolb, C. E., and Worsnop, D. R.: Development of an aerosol mass spectrometer for size and composition analysis of submicron particles, Aerosol Sci. Tech., 33, 49–70, 2000.

Jimenez, J. L., Jayne, J. T., Shi, Q., Kolb, C. E., Worsnop, D. R., Yourshaw, I., Seinfeld, J. H., Flagan, R. C., Zhang, X. F., Smith, K. A., Morris, J. W., and Davidovits, P.: Ambient aerosol sampling using the Aerodyne Aerosol Mass Spectrometer, J. Geophys. Res., 108, 8425, doi:10.1029/2001JD001213, 2003.

Krivácsy, Z., Hoffer, A., Sárvári, Z., Temesi, D., Baltensperger, U., Nyeki, S., Weingartner, E., Kleefeld, S., and Jennings, S. G.: Role of organic and black carbon in the chemical composition of atmospheric aerosol at European background sites, Atmos. Env., 35, 6231–6244, 2001.

Marcolli, C. and Krieger, U. K.: Phase changes during hygroscopic cycles of mixed organic/inorganic model systems of tropospheric aerosols, J. Phys. Chem., A110, 1881–1893, 2006.

McFiggans, G., Alfarra, M. R., Allan, J., Bower, K., Coe, H., Cubison, M., Topping, D., Williams, P., Decesari, S., Facchini, C., and Fuzzi, S.: Simplification of the representation of the organic component of atmospheric particulates, Faraday Discuss., 130, 341–362, 2005.

McFiggans, G., Artaxo, P., Baltensperger, U., Coe, H., Facchini, M., Feingold, G., Fuzzi, S., Gysel, M., Laaksonen, A., Lohmann, U., Mentel, T., Murphy, D., O'Dowd, C., Snider, J., and Weingartner, E.: The effect of physical and chemical aerosol properties on warm cloud droplet activation, Atmos. Chem. Phys., 6, 2593–2649, 2006,
http://www.atmos-chem-phys.net/6/2593/2006/.

Mikhailov, E., Vlasenko, S., Niessner, R., and Pöschl, U.: Interaction of aerosol particles composed of protein and salts with water vapor: hygroscopic growth and microstructural rearrangement, Atmos. Chem. Phys., 4, 323–350, 2004,
http://www.atmos-chem-phys.net/4/323/2004/.

Peng, C., Chan, M. N., and Chan, C. K.: The hygroscopic properties of dicarboxylic and multifunctional acids: Measurements and UNIFAC predictions, Env. Sci. Tech., 35, 4495–4501, 2001.

Putaud, J. P., Raes, F., Van Dingenen, R., Brüggemann, E., Facchini, M. C., Decesari, S., Fuzzi, S., Gehrig, R., Hüglin, C., Laj, P., Lorbeer, G., Maenhaut, W., Mihalopoulos, N., Mülller, K., Querol, X., Rodriguez, S., Schneider, J., Spindler, G., ten Brink, H., Trseth, K., and Wiedensohler, A.: European aerosol phenomenology-2: chemical characteristics of particulate matter at kerbside, urban, rural and background sites in Europe, Atmos. Env., 38, 2579–2595, 2004.

Reilly, P. J. and Wood, R. H.: Prediction of properties of mixed electrolytes from measurements on common ion mixtures, J. Phys. Chem., 73, 4292–4297, 1969.

Saxena, P., Hildemann, L. M., McMurry, P. H., and Seinfeld, J. H.: Organics alter hygroscopic behavior of atmospheric particles, J. Geophys. Res., 100, 18 755–18 770, 1995.

Stokes, R. H. and Robinson, R. A.: Interactions in aqueous nonelectrolyte solutions. I. Solute-solvent equilibria, J. Phys. Chem., 70, 2126–2130, 1966.

Swietlicki, E., Zhou, J. C., Berg, O. H., Martinsson, B. G., Frank, G., Cederfelt, S. I., Dusek, U., Berner, A., Birmili, W., Wiedensohler, A., Yuskiewicz, B., and Bower, K. N.: A closure study of sub-micrometer aerosol particle hygroscopic behaviour, Atmos. Res., 50, 205–240, 1999.

Topping, D. O., McFiggans, G. B., and Coe, H.: A curved multicomponent aerosol hygroscopicity model framework: Part 1 - Inorganic compounds, Atmos. Chem. Phys., 5, 1205–1222, 2005a.

Topping, D. O., McFiggans, G. B., and Coe, H.: A curved multicomponent aerosol hygroscopicity model framework: Part 2 – Including organic compounds, Atmos. Chem. Phys., 5, 1223–1242, 2005b.

Weingartner, E., Burtscher, H., and Baltensperger, U.: Hygroscopic properties of carbon and diesel soot particles, Atmos. Env., 31, 2311–2327, 1997.

Zdanovskii, A.: New methods for calculating solubilities of electrolytes in multicomponent systems, Zhur. Fiz. Khim., 22, 1475–1485, 1948.

Zhang, Q., Alfarra, M. R., Worsnop, D. R., Allan, J. D., Coe, H., Canagaratna, M. R., and Jimenez, J. L.: Deconvolution and quantification of hydrocarbon-like and oxygenated organic aerosols based on aerosol mass spectrometry, Env. Sci. Tech., 39, 4938–4952, 2005a.

Zhang, Q., Worsnop, D. R., Canagaratna, M. R., and Jimenez, J. L.: Hydrocarbon-like and oxygenated organic aerosols in Pittsburgh: insights into sources and processes of organic aerosols, Atmos. Chem. Phys., 5, 3289–3311, 2005b.

Zhang, Q., Jimenez, J. L., Canagaratna, M. R., Allan, J. D., Coe, H., Ulbrich, I., Alfarra, M. R., Takami, A., Middlebrook, A. M., Sun, Y. L., Dzepina, K., Dunlea, E., Docherty, K., DeCarlo, P. F., Salcedo, D., Onasch, T., Jayne, J. T., Miyoshi, T., Shimono, A., Hatakeyama, S., Takegawa, N., Kondo, Y., Schneider, J., Drewnick, F., Borrmann, S., Weimer, S., Demerjian, K., Williams, P., Bower, K., Bahreini, R., Cottrell, L., Griffin, R. J., Rautiainen, J., Sun, J. Y., Zhang, Y. M., and Worsnop, D. R.: Ubiquity and dominance of oxygenated species in organic aerosols in anthropogenically-influenced Northern Hemisphere midlatitudes, Geophys. Res. Lett., 34, L13801, doi:10.1029/2007GL029979, 2007.